

PhD Thesis

Modern imaging of normal and pathological conditions of the hip and knee joints with special focus on the EOS 2D/3D system

Kinga Szuper M.D.



University of Pécs
Medical School
Pécs
2024

PhD Thesis

Modern imaging of normal and pathological conditions of the hip and knee joints with special focus on the EOS 2D/3D system

Kinga Szuper M.D.

Clinical Medical Sciences

Program leader and supervisor: Prof. Péter Than, M.D., Ph.D.

Co-supervisor: Gábor Horváth M.D., Ph.D.

Head of Doctoral School : Prof. Lajos Bogár, M.D., Ph.D.,D.Sc.



University of Pécs
Medical SchoolC
Pécs
2024

Table Of Contents

ABBREVIATIONS USED	2
1. INTRODUCTION	3
2. IMAGING METHODS USED IN ORTHOPEDIC PRACTICE.....	3
3. EOS 2D/3D ULTRA-LOW DOSE DIGITAL IMAGING.....	5
4. RELEVANCE OF TRADITIONAL X-RAY EXAMINATION IN ORTHOPEDIC PRACTICE.....	5
5. THE RELEVANCE OF MRI IN ORTHOPEDIC PRACTICE.....	7
6. ANATOMICAL DESCRIPTION OF THE LOWER LIMB USING EOS IMAGING	10
7. DISCUSSION.....	19
8. NEW FINDINGS	20
PUBLICATIONS RELATED THIS THESIS	22
OTHER PUBLICATIONS RELATED TO THIS THESIS	23
ACKNOWLEDGMENTS	24

Abbreviations used

AP – anteroposterior

CD angle – collodiaphyseal angle

CT – computed tomography

EOS – extended orthopedic system

HHS – Harris Hip Score

HKA – hip-knee-ankle angle

HKS – hip-knee shift

MR/MRI – magnetic resonance imaging

US – ultrasound

1. Introduction

With the development of radiological imaging, new diagnostic methods have emerged in musculoskeletal diagnostics, which have become increasingly important alongside orthopedic physical examinations in recent times. The use of imaging examinations significantly contributes to establishing an accurate diagnosis of orthopedic conditions and assists in determining the appropriate surgical indications. Today, we have several advanced examination methods at our disposal, such as traditional X-rays, ultrasound, EOS, CT, and MRI, from which we can choose based on the following criteria: specificity, efficiency, radiation exposure risk, cost, and duration. While these examinations facilitate daily medical work, they can also lead to the over- or under-diagnosis of certain conditions.

2. Imaging methods used in orthopedic practice

The earliest examination method was X-ray, discovered by Wilhelm Conrad Röntgen in 1895. Initially, it was used in the diagnosis of internal diseases, such as detecting kidney stones and performing chest and lung X-rays. Today, its main application is in diagnosing bone and joint disorders, as well as in surgical planning and post-operative follow-up examinations. Its most important advantages in daily practice are its widespread availability, speed, and low cost, while its drawback is that it does not allow for 3D imaging.

Ultrasound is a widely accessible, inexpensive examination method that carries no health risks. Animal experiment observations and its physical description date back to the 1790's, but the first human examinations did not take place until 1942. Initially, it was used to observe brain tumors and ventricles, and later in abdominal and pelvic diagnostics. Its musculoskeletal application was first noted much later, in 1958. Ultrasound is a valuable diagnostic tool for evaluating tendons, muscles, and ligaments. It is also suitable for detecting joint effusions (such as hydrops or hemarthrosis) and cysts. In daily orthopedic practice, ultrasound is most commonly performed for knee and shoulder joint disorders and chronic injuries.

While the previously mentioned diagnostic methods only allowed for 2D imaging, CT and MRI, which will be discussed now, make 3D imaging possible:

The development of the theoretical background for CT is linked to Cormack. The first CT machine was invented by Hounsfield in 1968, who replaced the earlier X-ray tube with a gamma radiation source, allowing for the examination of living tissues. The first human tomographic examination was performed in 1971 on a woman suspected of having a brain tumor.

In particularly difficult situations, such as revision surgeries or complex primary cases requiring prostheses, CT provides more accurate morphological imaging compared to traditional X-rays. With the available 3D reconstruction, intraoperative challenges can be predicted in advance. Its advantages include being relatively fast, accessible, and providing true spatial imaging due to the 3D reconstruction, which is more detailed compared to X-rays. However, its radiation exposure is approximately 300 times that of an X-ray.

In daily patient care, MRI is used to evaluate joints and surrounding soft tissues. The principle of magnetic resonance, which underpins MRI, was described in 1946, but the first human examination did not take place until 1977. Initially, MRI was primarily used in brain diagnostics and the extensive study of tumors and infections. Later, it gained increasing importance in musculoskeletal imaging. One of its advantages is that it can diagnose cartilage damage non-invasively at such an early stage that irreversible joint damage can still be prevented. In daily orthopedic practice, MRI is mainly used to detect abnormalities in joints, muscles, tendons, and ligaments. Its most common applications are in diagnosing soft tissues around and within the shoulder, hip, and knee.

3. EOS 2D/3D ultra-low dose digital imaging

The EOS 2D/3D ultra-low dose digital X-ray device uses micro-fiber gas detectors discovered by Charpack for imaging. During an EOS examination, two X-ray tubes placed perpendicular to each other, along with their corresponding gas detectors, move vertically to simultaneously capture an AP (anteroposterior) and a lateral image of the entire body.

One of its advantages is that it captures images of the whole body in a standing (weight-bearing) position, allowing for the determination of mechanical parameters. This is achieved with a short imaging time and low radiation exposure. Another benefit of the system is that, with the SterEOS 3D software package, 3D reconstruction can be performed afterward, enabling the determination of spatial geometrical parameters. The system was initially used in the diagnosis of scoliosis and for determining the geometrical parameters of the lower limbs, but its range of applications is continually expanding. Nowadays, publications are emerging regarding its use in assessing the postoperative positioning of knee and hip prostheses and in preoperative planning. The new "microdose" protocol provides further opportunities to reduce the emitted radiation dose, with international studies highlighting its significance, particularly in monitoring the progression of idiopathic scoliosis.

4. Relevance of traditional X-ray examination in orthopedic practice

4.1. Our objectives in evaluating traditional X-ray images were as follows:

1. To demonstrate the radiological forms of dysplastic coxarthrosis. Using case studies, I aimed to present the prosthetic options appropriate to the degree of joint destruction.
2. To showcase the late radiological consequences of a knee prosthesis implanted in an inappropriate position.
3. To review the radiological results of cementless revisions, with particular emphasis on the frequency of heterotopic bone formation.

4.2. Method of evaluating traditional X-ray images

To demonstrate the orthopedic applicability of traditional X-ray examinations, we compared and evaluated the preoperative and immediate postoperative two-directional X-ray images of three patients who underwent hip prosthesis implantation due to dysplasia.

In our case report titled *Aseptic loosening and revision of a total knee prosthesis implanted in inappropriate position*, we analyzed and compared the immediate postoperative and follow-up X-ray images of a patient who underwent TKA (total knee arthroplasty) due to knee osteoarthritis.

In examining para-articular ossification, we reviewed the data of 58 patients who underwent surgery with cementless implants for aseptic loosening in our institute between 2000 and 2003. The follow-up examinations occurred on average 44 months (range: 30-52 months) post-operatively. Of the recalled patients, 26 returned (13 women, 13 men). AP X-ray images were taken of each patient's hip, which were compared to the postoperative images. The Brooker classification was used to determine the degree of para-articular ossification.

4.3. Results

The most common procedure performed in orthopedic departments is hip prosthesis implantation. Standard two-directional X-rays are essential for surgical planning. In our study, we examined dysplastic coxarthrosis, a late complication of hip dysplasia, and its radiological appearance. We presented the pre- and postoperative X-rays of three patients where special technical challenges had to be addressed during the primary implantation. In these surgeries, small and/or specially shaped prosthesis stems were implanted.

Regarding the radiological evaluation of knee prostheses, we demonstrated, through a case study, the early and late consequences of component malpositioning. The femoral and tibial components were implanted in inappropriate positions, compensating for each other's misalignment. X-ray examination performed three years after the surgery showed slight resorption around the tibial component. At the 10-year follow-up, there was marked loosening and tilting of the tibial component with significant bone loss, along with a break in the tibial lateral cortex. The lateral view also showed loosening of the femoral component.

In our examination of para-articular ossification, we reviewed the X-rays of 58 patients who underwent cementless revision for aseptic loosening in our institute between 2000 and 2003. During radiological follow-up, no signs of aseptic loosening were observed, but in 10 patients (38.46%), para-articular ossification was visible on follow-up X-rays, which had not been present on the postoperative images. In these patients, the acetabular component was revised in 7 cases, the stem in 2 cases, and both components in 1 case. Allograft acetabular reconstruction was performed in 8 cases, and femoral allograft spongiosa reconstruction in 1 case. In patients

with para-articular ossification, an average of 24 months (12 to 52 months) had passed since the revision surgery. The degree of ossification ranged from Grade 1 to 3 according to the Brooker classification. Among the 10 patients, 1 had Grade 1, 3 had Grade 2, and 6 had Grade 3 para-articular ossification.

We also reported a significant rate of para-articular ossification during the radiological follow-up of primary hip surgeries. The Corail stems showed excellent mid-term results regarding aseptic loosening, but due to the hydroxyapatite coating, we observed an increased rate of ossification. Of the 57 patients, 7 cases (12.28%) showed significant para-articular ossification, ranging from Grade 2 to 3 according to the Brooker classification, which was not visible on the postoperative X-rays.

5. The relevance of MRI in orthopedic practice

5.1. Objectives in presenting the utilization of MRI:

1. To determine the diagnostic reliability of MRI in knee injuries of various origins by comparing MRI findings with arthroscopy results.
2. To diagnose rare knee joint abnormalities, with a focus on the radiological examination of medial discoid meniscus.
3. To present two rare entities: lateral meniscus cyst and intra-articular ganglion.

5.2. Methods used in orthopedic MRI applications

In examining the diagnostic reliability of MRI, we reviewed the data of 327 patients at our institution between 2010 and 2013, with preoperative MRI performed in 110 cases. The gender distribution of these 110 patients was as follows: 45 males and 65 females, with an average age of 37 years (ranging from 21 to 53). All MR scans were conducted at the Pécs Diagnostic Center using Siemens Magnetom 1.5 and 3 Tesla MR machines.

In the case report titled *Medial discoid meniscus: A rare knee joint entity*, we conducted X-ray and MRI examinations on a 35-year-old female patient, followed by a diagnostic arthroscopy. We analyzed the imaging results and compared them with the arthroscopic findings. Since the

MRI did not initially report the presence of a medial discoid meniscus, we had the results re-evaluated by radiologists.

In our publication on *Differential diagnosis of lateral cystic lesions near the knee*, we reviewed and compared preoperative X-ray and MRI scans of a patient with a lateral meniscus cyst and another patient with a ganglion cyst, alongside the results of diagnostic arthroscopy.

5.3. Results of our MRI studies in daily orthopedic practice

In our investigation of the diagnostic reliability of MRI for knee joint assessments, we aimed to evaluate the accuracy of MRI reporting. We analyzed 110 patients who underwent arthroscopy following MRI. The arthroscopic findings included: 52 medial meniscus tears, 12 lateral meniscus tears, 39 anterior cruciate ligament (ACL) tears, 1 case of osteochondritis dissecans, 1 medial discoid meniscus, and 1 case of villonodular synovitis.

Post-operatively, we compared the MRI findings with the arthroscopic results, categorizing them based on agreement or disagreements. Our findings revealed that there was an agreement between MRI and arthroscopy in 68% of cases. In 15% of cases, the abnormalities described by MRI could not be confirmed, or a different lesion was identified. In the remaining 17%, only part of the abnormalities reported by MRI were confirmed by arthroscopy.

The most common knee injury was medial meniscus tears, which were confirmed by both MRI and subsequent arthroscopic examination in 52 cases. In a smaller number of cases (15), MRI reported a positive finding while arthroscopy was negative. Additionally, there were 8 instances where MRI did not identify the tear. We calculated the sensitivity and positive predictive value of MRI for medial meniscus injuries, yielding values of 86.66% and 77.61%, respectively. ACL tears were less frequently observed and were usually associated with medial meniscus injuries. For this injury type, MRI sensitivity was recorded at 81.25%, with a positive predictive value of 86.66%. Lateral meniscus tears were significantly less frequently described by MRI, reflecting their rarity. For lateral meniscus tears, MRI sensitivity and positive predictive value were 70.58% and 54.54%, respectively. We believe that the indication for MRI should be based on unclear physical symptoms, complex knee injuries, and rare abnormalities.

We highlighted the diagnostic challenges of rare knee joint conditions through the case of a 35-year-old female patient with persistent left medial knee complaints for several years. She reported no trauma prior to her symptoms and had undergone physiotherapy and a course of

oral chondroitin sulfate treatment at a rheumatology clinic. Physical examination revealed a 10-degree extension lag in the left knee, with flexion possible up to 140 degrees. The medial joint compartment was notably tender, and pain increased during rotational tests. Following the clinical examination protocol, we conducted two-directional X-rays, which did not reveal any structural bone abnormalities. Based on her subjective and clinical symptoms, suspicion of a medial meniscus tear led to an MRI for a more accurate diagnosis. The MRI indicated degenerative tearing of the medial meniscus with a parameniscal cyst, but did not report a discoid meniscus. After the surgery, we requested a revision of the MRI report, which then clearly described the discoid meniscus abnormality. Based on the clinical and radiological findings, we performed an arthroscopic procedure, during which we found a complete medial discoid meniscus with a large, lobular tear starting from its posterior section. We surgically removed the torn pieces and reshaped the meniscus into a normal C form using a shaver.

MRI is crucial not only in diagnosing rare lesions but also in differentiating soft tissue abnormalities around the knee. Cystic lesions near the knee joint can pose diagnostic challenges for orthopedic surgeons and occasionally for radiologists. The most commonly encountered cystic lesions in the knee include meniscus cysts and ganglion cysts. In our study, we examined both lateral meniscus cysts and intra-articular ganglion cysts. Clinically, a lateral meniscus cyst presents as a relatively firm soft tissue mass located above the lateral joint compartment, beneath the iliotibial tract attachment. In rare cases, as noted in our report, X-rays may reveal bone erosion corresponding to the mass on the lateral condyle of the tibia. The MRI performed for diagnosis clearly showed a meniscus cyst originating from the lateral joint space that eroded the tibial condyle. Ganglion cysts cannot be easily distinguished from other cystic lesions of the knee based on clinical appearance; they may also present as lateral soft tissue masses. X-rays do not typically reveal radiological abnormalities either. Our final diagnosis was confirmed by MRI, which demonstrated a multilocular ganglion cyst in the subcutaneous fat tissue ventrolaterally, as well as in Hoffa's fat pad and within the layers of the lateral retinaculum. Additionally, two joint free bodies likely originating from patellar cartilage were described in association with the ganglion cyst.

6. Anatomical description of the lower limb using EOS imaging

6.1. Objectives of the EOS imaging of the lower limb

1. Measurement of anatomical and biomechanical parameters:
The primary objective is to measure the normal anatomical and biomechanical parameters of the lower limb in both pediatric and adult age groups using the EOS 2D/3D method.
2. Establishment of population-related reference values:

Degenerative and traumatic conditions of the lower limb

1. Determination of anatomical and biomechanical parameters in a small patient population with coxarthrosis and gonarthrosis using the EOS 2D/3D method.
2. Precise measurement of limb length, axis, and rotation in our patients who have suffered lower limb fractures.

6.2. Method of EOS examination in healthy children

In our institute, we reviewed EOS examinations conducted between 2007 and 2012 among a population of children aged 4 to 16 years. Out of 716 examinations, we selected 508 images in which growth-affecting disorders could be excluded.

These 508 examinations were performed due to mild or moderate scoliosis, functional kyphosis, chondromalacia patellae, and idiopathic joint pain. The Risser sign was used for estimating skeletal maturity, and age groups were formed based on the patients' ages.

We performed a complete 3D reconstruction of both lower limbs, resulting in a total of 1016 limb models. During our investigation, we determined the parameters of the femur, as shown in Figure 1, and the parameters of the pelvis, as shown in Figure 2.

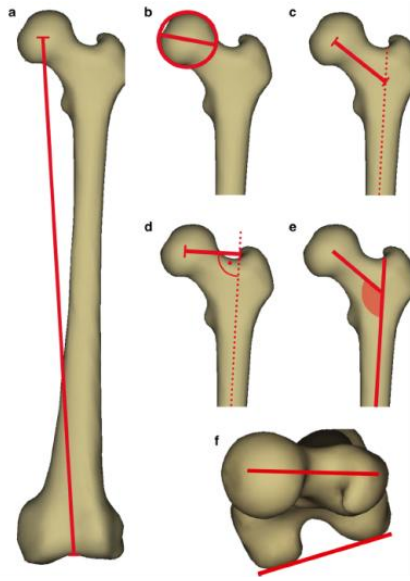


Figure 1: Anatomical parameters of the femur

a. Femoral mechanical axis length **b.** Femoral head diameter
c. neck length, **d.** Femoral offset, **e.** Collodiaphyseal angle,
f. Femoral torsion

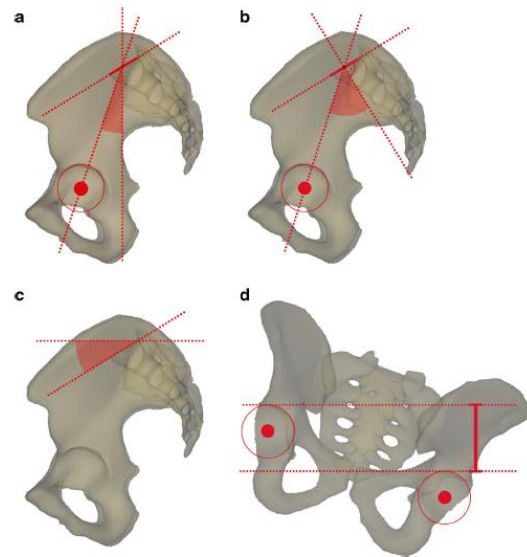
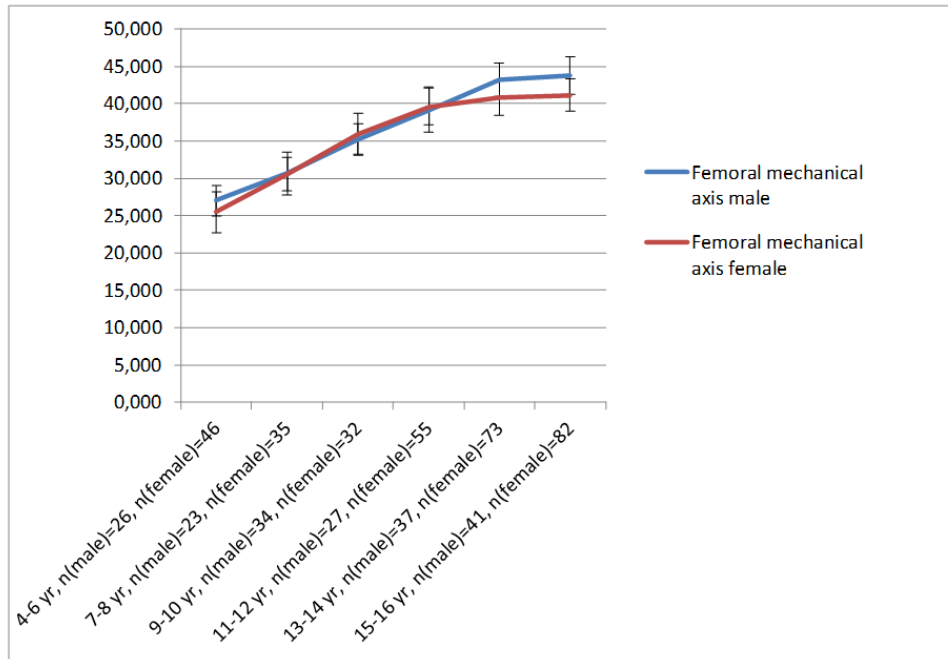


Figure 2: Anatomical parameters of the pelvis

a. Sagittal pelvic tilt **b.** Pelvic incidence, **c.** Sacral slope, **d.** Lateral pelvic tilt

6.3. Normal lower limb anatomy in childhood

By averaging the results of the studied population of children aged 4 to 16 years, we obtained characteristic normal geometric femur and pelvic parameters for childhood, which are illustrated in Figures 3-6. Except for the sagittal pelvic tilt, all examined parameters showed significant correlation with age. The sagittal pelvic tilt exhibited the same value across all age groups. No parameters showed any correlation with laterality; therefore, we calculated the average of both sides for further analysis.



3. Figure: Mechanical axis length of the femur in childhood by age group based on EOS measurements.

In Figure 3, it is clearly shown that the mechanical axis length of the femur significantly increases with age and gender. Differences between male and female skeletons become pronounced after the age of 11, with boys exhibiting higher values at this age. In the age group of 4 to 16 years, the mechanical axis length of the femur in boys increases from 27.0 cm to 43.7 cm, while in girls, it increases from 25.5 cm to 41.2 cm.

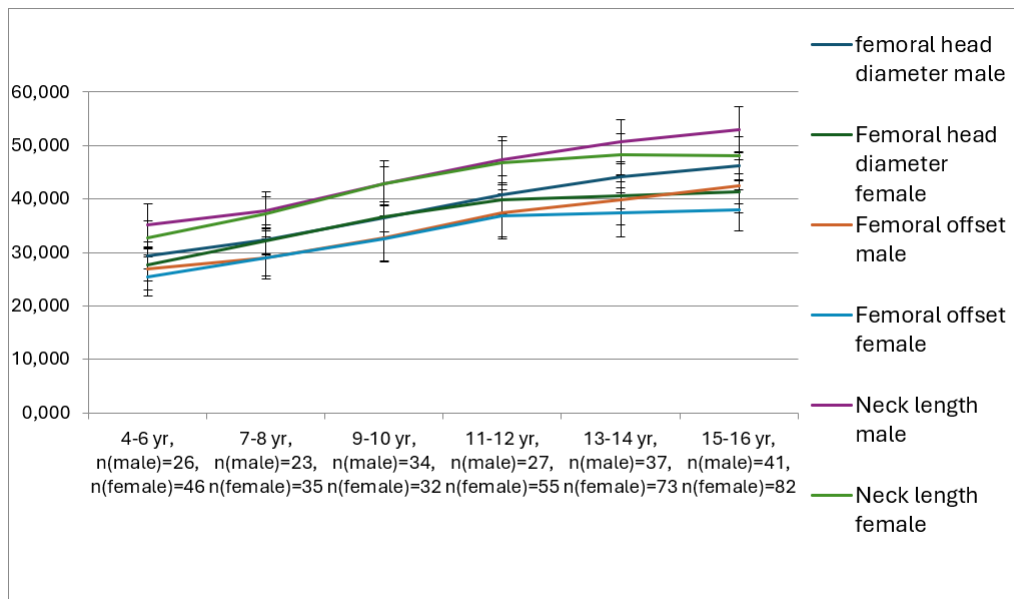
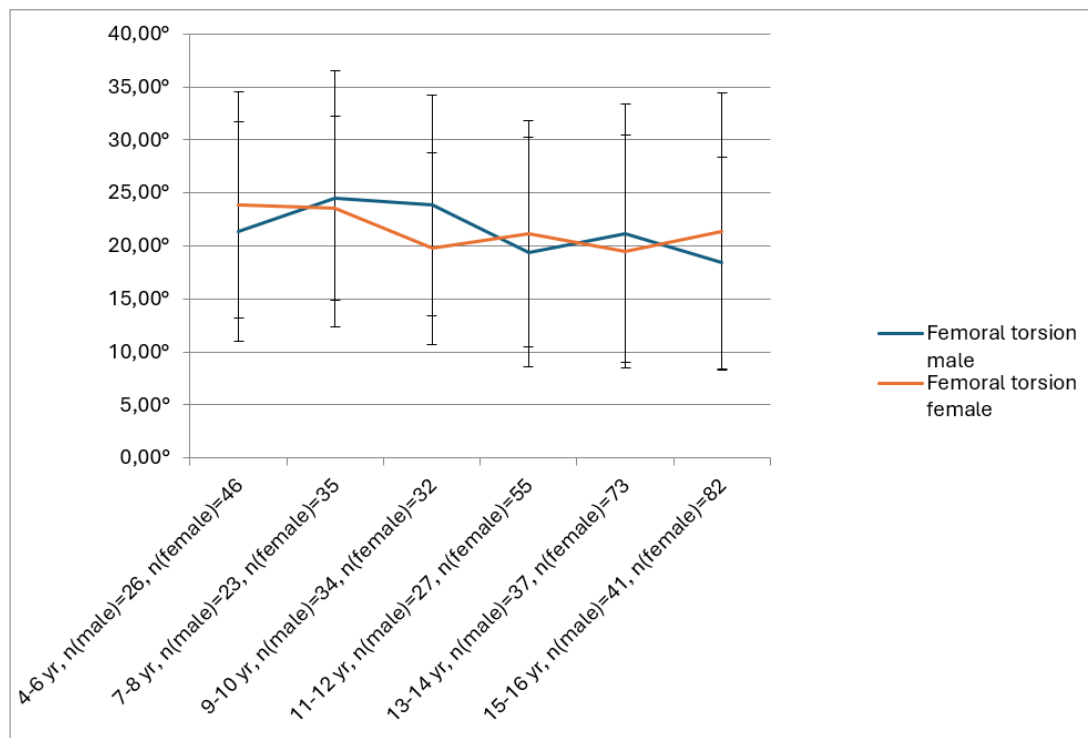


Figure 4: Proximal femur data by age group based on EOS measurements in childhood

Further statistically significant correlations were found between age and the femoral head diameter, neck length, and femoral offset. Differences between sexes were clearly evident in the femoral head diameter and neck length. In the 4-16 age group, boys showed an increase in femoral head diameter from 29.4 mm to 46.1 mm, while girls increased from 27.7 mm to 41.3 mm. The neck length for boys increased from 35.1 mm to 52.9 mm, whereas for girls, it increased from 32.8 mm to 48.1 mm.

The differences in femoral offset displayed fluctuating values up to the age of 12, after which significant growth was observed. The femoral offset for boys increased from 26.8 mm to 42.4 mm, while for girls, it changed from 25.5 mm to 37.9 mm (Figure 4).

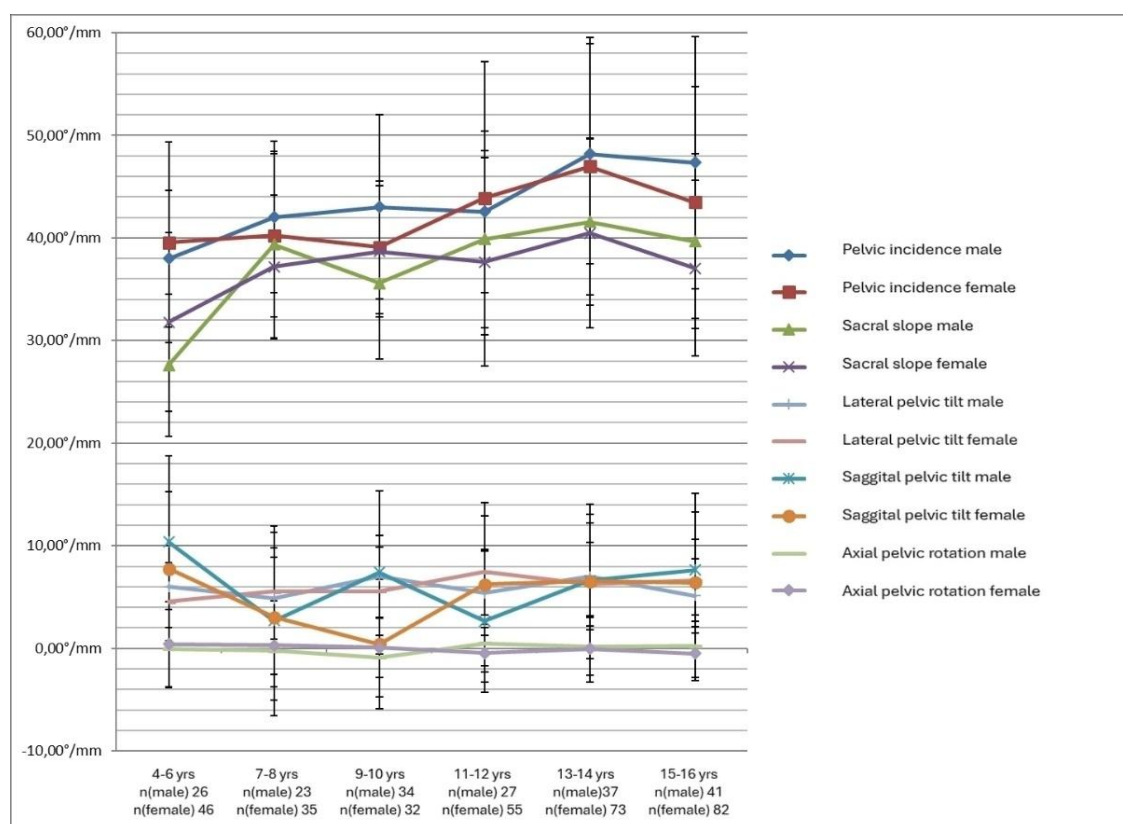


5. Figure: Femoral torsion in childhood based on EOS measurements by age group

The collodiaphyseal angle significantly changes with age. In boys, it decreases from 131.0° to 127.4°, while in girls, it reduces from 129.8° to 128.8°, showing no gender differences.

Additionally, a significant relationship was found between femoral torsion and age, but no inter-gender association was established. As children grow older, femoral torsion decreases from 21.4° to 18.4° in boys and from 23.9° to 21.4° in girls. It appears that there is greater inter-individual variability in this parameter (see Figure 5).

This data highlights the importance of monitoring these parameters during childhood development, as they may have implications for orthopedic assessment and interventions.



6. Figure: Pelvic parameters by age group based on EOS measurements in childhood

It can be observed that among the four pelvic parameters, only the sagittal pelvic tilt does not show a correlation with age; however, there are significant interindividual differences, with fluctuations around an average value of 6.4°. The parameters that correlate with age are as follows: the sacral slope increases from 29.6° to 39.7°, the pelvic incidence also shows an increasing trend from 39.09° to 44.4°, and the lateral pelvic tilt increases from 5.1 mm to 6.2 mm (Figure 6). None of the pelvic parameters show any correlation with gender. In children, anatomical differences between the pelvises of adult males and females cannot be confirmed either.

6.4. Methodology of EOS examination in healthy adults and adults with hip and knee osteoarthritis

In our institution, between 2008 and 2010, we conducted EOS 2D/3D examinations for the anatomical characterization of normal lower limbs. We based our study on 128 lower limb 3D reconstructions from 65 healthy adults. The average age of participants at the time of the scans

was 26.3 years (SD 19.39). According to the radiological staging classification described by Kellgren and Lawrence, these patients belonged to the normal group, indicating that there were no signs of osteoarthritis in either their hip or knee joints. Clinical outcomes were collected in an Excel spreadsheet, followed by statistical analysis using SPSS software.

For determining lower limb parameters in patients with osteoarthritis, we performed EOS 2D/3D examinations on 37 patients with coxarthrosis in our institution. Among the examined patients, 16 had bilateral hip involvement, resulting in a total of 53 hip joints being analyzed. The gender distribution was as follows: 28 females and 9 males. The average age of the patients at the time of the scans was 67.8 years (SD 45.80).

We also examined 32 patients with gonarthrosis, of which 18 had involvement in only one knee, while 14 had both knees affected, leading to a total of 46 knee joints being analyzed. The gender distribution during the examination was as follows: 28 females and 4 males, with an average age of 67 years (range 53-80). The degree of osteoarthritis, according to the Kellgren and Lawrence classification, showed a score of 2 or above in both the coxarthrosis and gonarthrosis groups, which was also confirmable via traditional X-ray imaging. As in previous studies, we determined the geometric parameters illustrated in Figure 1.

6.5. Geometric parameters of healthy adults and adults suffering from hip and knee joint osteoarthritis

By averaging the results from the sample derived from the healthy population aged between 19 and 39 years, we obtained the normal geometric parameters characteristic of young adulthood, which are presented in Table I.

Lenght parameteres	Total average	Standard deviation	Man	Women
Femur lenght (cm)	42,9	3,11	44,1	41,8
Tibia length(cm)	37,1	2,81	38	35,3
Total limb lenght (cm)	80,5	5,82	82,5	78,5
Proximal femur				
Femur head diameter (mm)	44,5	3,78	47,1	42
Femur neck lenght (mm)	50,5	4,65	52,7	48,8
Collodiaphyseal angle(°)	128,4	4,93	129	127,8
Knee				
Varus/ Valgus (°)	-0,8	3,13	-2,3	0,7
Flessum/ Recurvatum (°)	-1,2	7,37	1,2	-3,7
HKS (°)	4,8	1,33	4,9	4,6
Tibial mechanical angle(°)	88	3,57	86,4	89,6
Torsions				
Femoral torsion (°)	17,1	11,51	15,1	19,2
Femorotibial rotation (°)	2,3	7,16	0,9	2,6
Tibial torsion (°)	36	8,35	34,3	37,7

Table I: Values of normal lower limb parameters determined by EOS examination in adults

Based on the table, we drew the following conclusions: The length and diameter values, as well as the collodiaphyseal angle of males, are greater than those of females. The HKS (hip-knee-shaft) angle, which is the angle formed by the anatomical and mechanical axes of the femur in the frontal plane, showed an average of 4.8° with no significant gender differences.

The angle formed by the mechanical axes of the tibia and femur is known as the femorotibial axis angle. In the program, a varus position is represented as negative, while a valgus direction is positive. Based on the averages of the examined patients, the normal axis position is varus. Interestingly, in males, this parameter deviates more towards varus, while in the female group, it deviates towards valgus. When measuring the angle between the two mechanical axes in the sagittal plane, a flessum indicates values greater than 0, while a recurvatum indicates values

less than 0. The average showed a slight recurvatum. Here, too, there was a significant difference between the sexes, with women showing higher values.

The values of torsions were quite varied. The average torsion of the femoral neck was 17.1°, with women showing greater anteversion than men. The angle between the line touching the two most posterior points of the tibial plateau and the bimalleolar line in the plane perpendicular to the mechanical axis of the tibia defines tibial torsion. According to our measurements, its average value was 36°, which indicates significant external rotation. The average for the female group was also higher here than for the male group. The sterEOS 3D software calculates the femorotibial rotation based on the angle between the posterior bimalleolar line and the line touching the two most posterior points of the tibial plateau in a plane perpendicular to the mechanical axis of the femur. A positive value indicates external rotation of the tibia, while a negative value indicates internal rotation. The overall average was 2.3°, with the female average again exceeding the male.

The geometric parameters of the 37 patients with coxarthrosis and the 32 patients with gonarthrosis are summarized in Tables II and III.

Total hip(n=53)	Average	Standard deviation
Age (év)	67,8	29,5
Femur lenght (cm)	40,8	2,6
Tibia lenght (cm)	35,2	2,56
Total limb lenght (cm)	76	56,16
Femoral diameter (mm)	46	4,13
Femur neck length (mm)	50,8	4,83
Collodiaphyseal angle (°)	122,8	6,03
Femoral anterversion (°)	15,6	11,21
Femoro-tibial rotation (°)	2,2	7,2
Tibial torsion (°)	26,8	9,4

Table II: Geometric parameters in coxarthrosis hip cases (EOS examination of 53 hip joints in 37 patients)

Total knee (n= 46)	Average	Standard deviation
Age	67.0	12.73
Valgus/Varus (°)	-6.0	2.55
Flessum/Recurvatum (°)	7.0	6.44
HKS (°)	7.0	2.25
Tibial mechnaical angle (°)	85.2	3.41

Normal axis (n=7)	Average	Standard deviation
age	70.3	11,7
Valgus/Varus (°)	-0.9	1.86
Flessum/Recurvatum (°)	7.0	4.71
HKS (°)	6.4	2.38
Tibial mechnaical angle (°)	85.7	4.31

Varus axis (n=35)	Average	Standard deviation
age	69.1	29.9
Valgus/Varus (°)	-8.8	4.19
Flessum/Recurvatum (°)	8.8	7.52
HKS (°)	7.0	2.34
Tibial mechnaical angle (°)	85.0	3.31

Valgus axis (n=4)	Average	Standard deviation
Age	67.0	29.6
Valgus/Varus (°)	9.6	1.61
Flessum/Recurvatum (°)	5.2	7.09
HKS (°)	7.0	2.05
Tibial mechanical angle(°)	93.9	2.96

Table III: Geometric Parameters in Gonarthrosis Cases Assessed by EOS Examination

We compared our results with the data from the healthy population. The tables show that in patients with coxarthrosis, the average collodiaphyseal angle, anteversion, femur and tibia lengths, as well as the total limb length, are decreased compared to the normal population values. However, the femoral offset and femoral head diameter show higher values than the normal values. Based on our measurements, the length of the femoral neck does not seem to be affected by the disease.

In the case of patients with gonarthrosis, we classified them based on lower limb alignment, and I made the following observations: Among the examined patients, 7 had normal alignment, with an average of -0.9° , 35 had varus alignment, with an average of -8.8° , and the remaining 4 had valgus alignment, with an average of 9.6° . Our results indicate that the most common alignment in gonarthrosis is varus.

7. Discussion

Today, the most advanced imaging devices are widely available for daily patient care, significantly reducing the time required to reach a diagnosis and enabling targeted treatment to begin as soon as possible. In my scientific work, I aimed to provide a detailed overview of the imaging techniques accessible in daily orthopedic outpatient care, including X-rays, CT, MRI, and EOS examinations. I discussed the main operational principles of these devices and their applicability in the diagnosis of lower limb conditions. Through case studies, I tried to support how each examination method can provide additional information relative to the others and how they can assist in surgical planning. I reported on a new X-ray-based device that is unique in lower limb diagnostics and presented the three-dimensional geometric parameters characteristic of normal and pathological lower limbs in both children and adults.

8. New findings

8.1. In the application of traditional X-ray examination in orthopedi

8.1.1. Radiological evaluation of the prosthetic outcomes of dysplastic femurs

- In our publication, we presented case studies discussing the suitability of traditional prosthesis stems for the prosthetic treatment of dysplastic hip joints. This kind of report is novel in the domestic literature and follows well the international recommendations.

8.1.2. Radiological assessment of paraarticular ossification

- We were the first to publish the radiological results of cementless revision hip prostheses in the domestic literature.
- Contrary to the literature, we found high levels of paraarticular ossification, highlighting the need for preventive meas

8.1.3. Radiological analysis of knee prosthesis positioning

- In our case report, we emphasized the importance of correct positioning of the femoral component, the late consequences of concurrent malpositioning of the tibial component, and also discussed its revision possibilities.

8.2. In the clinical use of MRI diagnosis of the knee joint

- We were able to confirm the diagnostic reliability of MRI in cases of medial and lateral meniscus tears, as well as cruciate and collateral ligament ruptures; our results closely aligned with international literature.
- Uniquely in the domestic literature, we determined the sensitivity and positive predictive value of MRI in cases of medial and lateral meniscus tears and anterior cruciate ligament ruptures.
- We presented rare knee joint entities (medial discoid meniscus, lateral meniscus cyst, intra-articular ganglion), detailed the difficulties in MRI reporting, and reviewed international recommendations regarding their orthopedic management.

8.3. In the use of EOS for lower limbs

- We were the first to publish the role of EOS examination in the radiological assessment of the entire lower limb in both domestic and international literature.
- We measured parameters of normal and pathological hips and knees in young adults and compared our results with other international publications.
- We defined normal proximal femur and pelvic parameters for children using EOS examination.
- We validated the relevance of EOS examination in the control assessment of lower limb fracture fixation surgeries by measuring various length and rotational parameters.

Publications related this thesis

Szuper K, Giyab O, Than P. Térdközeli laterális cystosus elváltozások differenciál diagnosztikája. Orv Hetil 2019, 160:593-599. **IF:0,497**

Szuper K, Schlégl AT, Leidecker E, Vermes C, Somoskeőy S, Than P. Three-dimensional quantitative analysis of the proximal femur and the pelvis in children and adolescents using an upright biplanar slot-scanning X-ray system. Pediatr Radiol 2015, 45:411-421. **IF:1,57**

Szuper K, Rosta B, Than P, Bogner P, Hetényi Sz, Vermes Cs. Térdízületi MR vizsgálat ortopédiai diagnosztikai megbízhatósága M Traumatol 2015, 58:123-128.

Szuper K, Kuzsner J, Vermes Cs, Than P. A dysplasiás femur protetizálásának eltérő megoldási lehetőségei csípő TEP beültetések M Traumatol 2014, 57:57-63.

Szuper K, Dömse E, Nőt L, Somoskeőy Sz, Than P. Femur és tibia diaphysis törések műtétet követő vizsgálata EOS 2D/3D röntgenkészülékkel. M Traumatol 2013, 56:119-126.

Szuper K, Bogner P, Hetényi Sz, Vermes Cs, Than P. Ritka térdízületi entitás: mediális discoid meniscus. Esetismertetés M Traumatol 2013, 56:227-230.

Szuper K, Than P. Hidroxiapatit bevonatú cement nélküli csípőprotézis szárral elért középtávú eredmények klinikánkon M Traumatol 2012, 55:261-267.

Szuper K, Somoskeőy Sz, Than P, Illés T. EOS 2D/3D képalkotás alkalmazási lehetőségei az alsó végtagon. M Traumatol 2012, 55:203-212.

Szuper K, Horváth G, Bellyei Á, Than P. Cement nélküli implantátummal végzett csípőrevíziók eredményei különös tekintettel a heteretop csontképződésre. M Traumatol 2009, 52:37-44.

Other publications related to this thesis

Schlégl ÁT, **Szuper K**, Somoskeöy S, Than P. 3D radiological imaging of the normal lower limb alignment in children Int Orthop 2015, 39: 2073-2080. **IF:2,11**

Schlégl ÁT, **Szuper K**, Somoskeöy S, Than P. Az alsó végtag tengelyállásának vizsgálati lehetőségei. Tapasztalataink az új EOS 2D/3D technológiával. M Traumatol 2015, 58:131-143.

Schlégl Á, **Szuper K**, Somoskeöy Sz, Than P. Az EOS 2D/3D System alkalmazhatóságának vizsgálata a szabad alsó végtag anatómiai és biomechanikai paramétereinek mérésére gyermekkorban Orv Hetil 2014, 155:1701-1712. **IF:0,354**

Antal H, **Szuper K**, Than P. Nyakban rögzülő szárral végzett csípőízületi totál endoprotézis rövid távú eredményei klinikánkon. Két eset ismertetése. M Traumatol 2013, 56:233-239.

Than P, **Szuper K**, Somoskeöy Sz, Warta V, Illés T. Geometrical values of the normal and arthritic hip and knee detected with the EOS imaging system Int Orthop 2012, 36:1291-1297. **IF: 2,770**

Than P, **Szuper K**, Somoskeöy Sz. Hibás pozícióban beültetett totál térdprotézis aszeptikus lazulása és revíziója: Esetismertetés M Traumatol 2012, 55:79-84.

Acknowledgments

I would like to express my heartfelt gratitude first and foremost to Prof. Dr. Péter Than, my supervisor and the director of the Orthopedic Clinic at PTE ÁOK, who has continuously supported me since the beginning of my career and has assisted me in my clinical and scientific activities.

I am also very thankful to my co-supervisor, Dr. Gábor Horváth. His advice and insights derived from his professional experience have been an extraordinary help in writing this dissertation.

I owe thanks to my colleague Dr. Ádám Schlégl for his contributions to the publications.

Additionally, I would like to thank the staff and my colleagues at the PTE ÁOK Orthopedic Clinic, who assisted me in the preparation of various publications and in my daily work.

I am grateful to my family, who have stood by me with their love and understanding throughout my work.